

Molecular pathology of brain matrix metalloproteases, claudin5, and aquaporins in forensic autopsy cases with special regard to methamphetamine intoxication

Qi Wang · Takaki Ishikawa · Tomomi Michiue ·
Bao-Li Zhu · Da-Wei Guan · Hitoshi Maeda

Received: 20 December 2013 / Accepted: 21 January 2014 / Published online: 13 February 2014
© Springer-Verlag Berlin Heidelberg 2014

Abstract Methamphetamine (METH) is a highly addictive drug of abuse and toxic to the brain. Recent studies indicated that besides direct damage to dopamine and 5-HT terminals, neurotoxicity of METH may also result from its ability to modify the structure of blood-brain barrier (BBB). The present study investigated the postmortem brain mRNA and immunohistochemical expressions of matrix metalloproteases (MMPs), claudin5 (CLDN5), and aquaporins (AQPs) in forensic autopsy cases of carbon monoxide ($n=14$), METH ($n=21$), and phenobarbital ($n=17$) intoxication, compared with mechanical asphyxia ($n=15$), brain injury ($n=11$), non-brain injury ($n=21$), and sharp instrument injury ($n=15$) cases. Relative mRNA quantification using Taqman real-time PCR assay demonstrated higher expression of AQP4 and MMP9, lower expression of CLDN5 in METH intoxication cases and lower expression of MMP2 in phenobarbital intoxication cases. Immunostaining results showed substantial interindividual variations in each group, showing no evident

differences in distribution or intensity among all the causes of death. These findings suggest that METH may increase BBB permeability by altering CLDN5 and MMP9, and the self-protective system maybe activated to eliminate accumulating water from the extracellular space of the brain by up-regulating AQP4. Systematic analysis of gene expressions using real-time PCR may be a useful procedure in forensic death investigation.

Keywords Forensicmolecularp pathology · Methamphetamine intoxication · MMPs · CLDN5 · AQPs

Introduction

Methamphetamine (METH) is a highly addictive drug that acts as a central nervous system (CNS) stimulating recreational drug. METH abuse has become a serious social problem worldwide. METH-induced direct damage to dopamine and 5-HT terminals was conventionally assumed to play a crucial role in METH neurotoxicity [1]. Recently, a new concept of METH-induced brain damage was raised, resulting from its ability to increase the blood-brain barrier (BBB) permeability [2, 3], though the potential mechanism has not been fully clarified.

Matrix metalloproteinases (MMPs) are members of the metzincin group of proteases that degrade most components of the extracellular matrix (ECM) in a variety of physiological and pathophysiological conditions [4]. MMP2 and MMP9, also called gelatinases, have both positive and negative roles in the healthy and diseased CNS [5]. Claudin5 (CLDN5) is a key tight junction (TJ) protein that plays an important role in modulation of BBB permeability [6]. In addition, aquaporins (AQPs) are water channels that facilitate water transport from and to the CNS. AQP1 and AQP4 are presumed as major contributors to participate in brain water homeostasis [7]. Our

Electronic supplementary material The online version of this article (doi:10.1007/s00414-014-0972-6) contains supplementary material, which is available to authorized users.

Q. Wang (✉)
Department of Forensic Medicine, Southern Medical University,
No. 1838, Guangzhou 510515, Guangdong Province,
People's Republic of China
e-mail: wangqi1980@live.com

Q. Wang · T. Ishikawa · T. Michiue · H. Maeda
Department of Legal Medicine, Osaka City University Medical
School, Osaka, Japan

T. Ishikawa
Division of Legal Medicine, Faculty of Medicine, Tottori University,
Tottori, Japan

B.-L. Zhu · D.-W. Guan
Department of Forensic Pathology, China Medical University School
of Forensic Medicine, Shenyang, China

previous study suggested that systematic analysis of these markers may be useful to investigate the pathogenesis of brain damage involving brain edema after severe burns [8].

The present study analyzed the gene expressions of MMP2, MMP9, CLDN5, AQP1 and AQP4, using reverse transcription quantitative PCR (RT-qPCR), combined with immunohistochemical detections, to investigate the molecular pathology in the brains of forensic autopsy cases with special regard to METH intoxication.

Materials and methods

Sample collection

Human brains of medicolegal autopsy cases ($n=114$; within 48 h postmortem with a median of 21 h; survival time, <0.5–192 h with a median of <0.5 h) at our institute were examined. The cases comprised 81 males and 33 females, between 18 and 90 (median, 50) years of age. The causes of death were determined on the basis of autopsy examination, including macromorphological, histological, toxicological, and biochemical analyses, as follows: mechanical asphyxia (As, $n=15$; atypical hanging, $n=7$, manual/ligature strangulation, $n=8$), brain injury (injury-1, $n=11$), non-brain injury (injury-2, $n=21$), sharp instrument injury (injury-3, $n=15$), carbon monoxide (intoxication-1, $n=14$) [9], METH (intoxication-2, $n=21$), and phenobarbital (intoxication-3, $n=17$) intoxication. A thorough neuropathological analysis was performed as part of our routine investigation, and cases with any preexisting neurological pathologies were excluded in the present study. In brain injury cases, tissues distant from the primary lesions were selected. Details are shown in Table 1.

The sample collections and analyses described below were performed within the framework of our routine casework, following the autopsy guidelines (2009) and ethical guidelines (1997 and 2003) of the Japanese Society of Legal Medicine, approved by our institutional ethics committee.

Table 1 Case profiles ($p=114$)

Cause of death	<i>n</i>	Male/Female	Age, years (median)	Survival time, h (median)	PMI, h (median)
Control groups					
As	15	9/6	25–82 (64)	<0.5	9–37 (22)
Injury-1	11	8/3	29–71 (39)	<0.5	13–35 (18)
Injury-2	21	17/4	22–90 (56)	<0.5	11–41 (23)
Injury-3	15	13/2	27–65 (50)	<0.5	13–29 (16)
Intoxication groups					
Intoxication-1	14	10/4	18–75 (51)	<0.5–3(<0.5)	10–45 (22)
Intoxication-2	21	17/4	29–71 (48)	6–192 (6)	7–42 (25)
Intoxication-3	17	7/10	24–64 (41)	8–96 (12)	9–37 (28)
Total	114	81/33	18–90 (50)	<0.5–192 (<0.5)	5–46 (21)

PMI, estimated postmortem interval; As, mechanical asphyxia; Injury-1, brain injury; Injury-2, non-brain injury; Injury-3, sharp instrument injury; Intoxication-1, carbon monoxide; Intoxication-2, methamphetamine; Intoxication-3, phenobarbital

Toxicological analyses

Postmortem heart blood COHb saturation was analyzed using a CO-oximeter system (Hemoximeter OSM3, Radiometer, Westlake, OH) [10, 11].

Drug analytical procedures, including chemicals and reagents, sample preparation, and instrumental conditions were performed by gas chromatography/mass spectrometry, as described previously [12].

RT-qPCR

Since the most significant METH-induced morphological alterations of the BBB occur in the cortex [3], brain tissue samples were taken from consistent sites in the cortex of parietal lobe of the left cerebral hemispheres at autopsy. All samples were immediately submerged in 1 ml of RNA stabilization solution (RNAlater™, Ambion, Austin) and stored at -80°C until use. RNA extraction, cDNA synthesis, and RT-qPCR were performed as described previously [13], following the manufacturer's protocol. Three previously validated reference genes, PES1, POLR2A, and IPO8, were used for normalization [8, 13]. Details are shown in [Supplementary Material](#). RT-qPCR reactions were run in 96-well reaction plates with a StepOnePlus Real-Time PCR System (Applied Biosystems, Foster City, USA). The threshold cycle (Ct) was calculated by the instrument software automatically (threshold value at 0.2). Raw fluorescent data (normalized reporter values, Rn values) were also exported.

Amplification efficiency calculation and data normalization

Amplification efficiencies were calculated from raw fluorescent data (Rn values), using a completely objective and noise-resistant algorithm, Real-time PCR Miner program [14]. The Real-time PCR Miner is an objective method using calculations based on the kinetics of individual PCR reactions without the need of the standard curve. The arithmetic mean value

of amplification efficiencies of each gene was used for data normalization.

Raw Ct values of targets and three previously validated reference genes, PES1, POLR2A, and IPO8 [8, 13], were imported into the qBase^{plus} software [15]. The qBase^{plus} algorithm takes amplification efficiencies into account, which distinguishes it from the $2^{-\Delta\Delta Ct}$ method [15–17]. Using a calibrator case (acute death due to ligature strangulation, 64-year-old male; 21 h postmortem), calibrated normalized relative quantity (CNRQ) values were exported from the qBase^{plus} software and statistically investigated. The calibrator case was selected randomly from the control group (As group), and the outcome will not change no matter which calibrator was selected.

Immunostaining

Paraffin-embedded brain tissue specimens were taken from the standardized anatomical regions [9, 18, 19]. Serial sections (5 μ m thick) were cut and stained with hematoxylin-eosin (HE) as part of routine laboratory investigation. In the present study, parietal lobes of left cerebral hemispheres were used for immunostaining.

Rabbit polyclonal anti-MMP2 antibody (Abcam, Cambridge, code ab79781, diluted 100-fold), rabbit polyclonal anti-MMP9 antibody (Abcam, Cambridge, code ab38898, diluted 800-fold), rabbit polyclonal anti-CLDN5 antibody (Abcam, Cambridge, code ab53765, diluted 500-fold), mouse monoclonal anti-AQP1 antibody (Abcam, Cambridge, code ab9566, diluted 500-fold), and rabbit polyclonal anti-AQP4 antibody (Santa Cruz Biotechnology, Santa Cruz, code sc-20812, diluted 500-fold), were used.

Following overnight incubation with the primary antibodies described above at room temperature, immunoreactions were visualized by the polymer method (ChemMate Envision, Dako, Tokyo, code k5027), and color was developed with 3,3'-diaminobenzidine tetrahydrochloride (DAB liquid system, Dako, Tokyo, code k3466), according to the manufacturer's instructions (counterstaining with hematoxylin).

Statistics

Correlation analyses between pairs of parameters were performed using Spearman's rho. The Kruskal-Wallis test, a non-parametric test for more than two independent samples, was used to compare groups, followed by multiple pairwise comparisons using the Steel-Dwass-Critchlow-Fligner procedure [20, 21]. These analyses were carried out using XLSTAT 2012 (Addinsoft, Paris, France) and StatView (version 5.0; SAS Institute Inc., Cornelius, NC, USA). A *p* value less than 0.05 was considered significant. The line in each box represents the median, and the lines outside each box represent the 90 % confidence interval in Fig. 1.

Results

Gene expression

The amplification efficiencies (mean values) of targets and reference genes ranged from 88.6 % (CLDN5) to 105.9 % (IPO8), showing small inter-individual variations (standard deviation, SD <5 %), which were similar to our previous study [8]. Details are shown in [Supplementary Material](#).

There were no gender-related differences, or age, or post-mortem interval, or survival time dependence in MMP2 and MMP9, CLDN5, AQP1, and AQP4 CNRQ values on Spearman's rho ($R^2 < 0.2$, $p > 0.05$). In As group, there is no statistical difference in CNRQ values of all markers between atypical hanging and manual/ligature strangulation ($p > 0.05$).

CNRQ values of MMP2 were evidently lower in phenobarbital intoxication group than in other groups (Fig. 1a). Higher MMP9 and AQP4 but lower CLDN5 mRNA expression levels were detected in METH intoxication cases (Fig. 1b, e, c). However, there was no significant difference in CNRQ values of AQP1 among all groups (Fig. 1d).

Immunostaining

Immunostaining showed substantial interindividual variations in each group. MMP2 was detected clearly in the neurons of cerebral cortex (Fig. 2a, b). MMP9 was weakly located in capillary endothelia (Fig. 2c, d). CLDN5 was strongly positive in capillary endothelia (Fig. 2e, f). AQP1 (Fig. 2g, h) and AQP4 (Fig. 2i, j) were mainly detected in glial cells which were morphologically identified as astrocytes. However, no significant differences in distribution or intensity were detected among the causes of death, including METH and phenobarbital intoxication cases.

Discussion

In forensic casework, postmortem diagnosis of death due to functional deterioration, including fatal intoxication, is sometimes difficult because of poor or nonspecific pathological findings. Diagnosis of fatal intoxication mainly depends on toxicological analyses. In such cases, investigation of characteristic functional changes of life-supporting organs may help to reinforce toxicological and pathological findings, excluding the contribution of any other traumas and diseases to the death process [22, 23].

Forensic science has made great strides in the last decade. More recently, RT-qPCR, using postmortem autopsy materials, has become a hotspot in the field of forensic pathology [17, 24–27]. Though there are several limitations to this technique, RT-qPCR can investigate the systemic pathophysiological

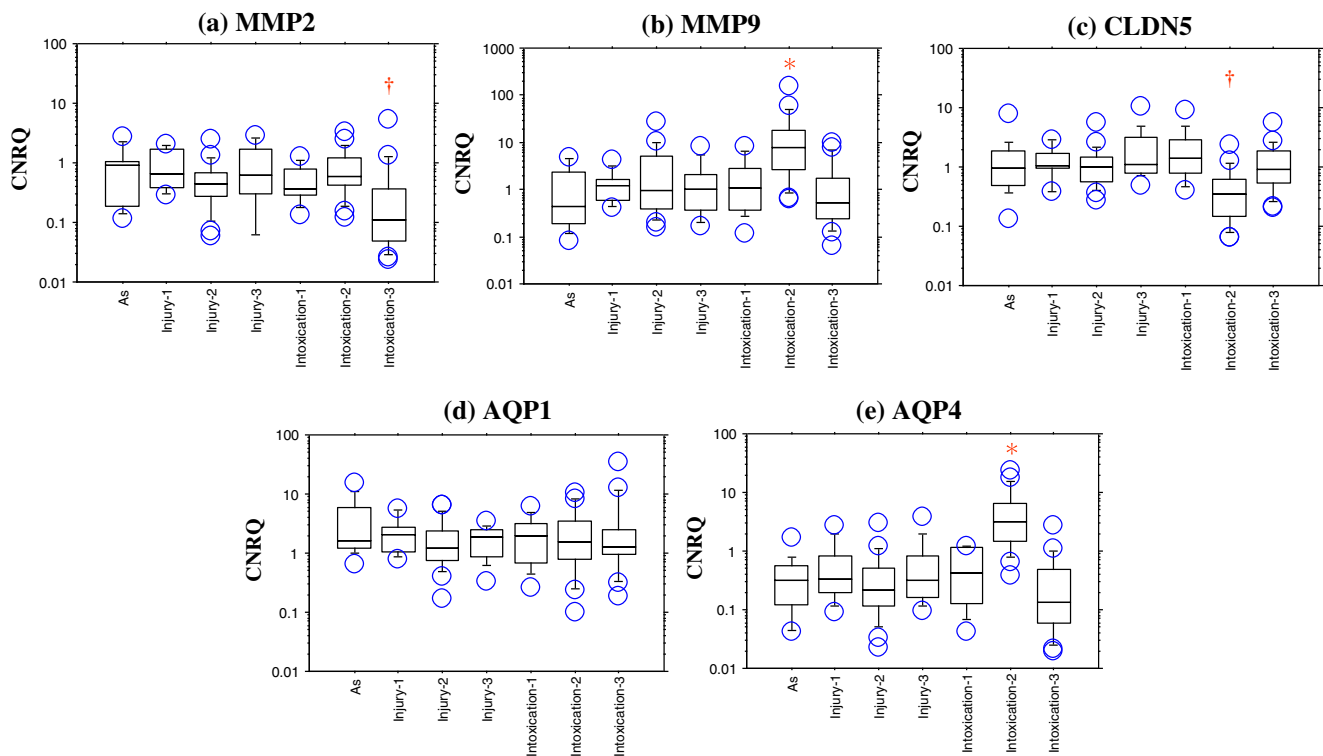


Fig. 1 CNRQ values of MMP2 (a), MMP9 (b), CLDN5 (c), AQP1 (d) and AQP4 (e) with regard to causes of death. **a** Significant difference was detected on Kruskal-Wallis (K-W) test ($p < 0.05$): †significantly lower ($p < 0.05$), intoxication-3 vs. other groups on Steel-Dwass-Critchlow-Fligner procedure. **b** and **e** Significant difference was detected on K-W test ($p < 0.05$): *significantly higher ($p < 0.05$), intoxication-2 vs. other groups on Steel-Dwass-Critchlow-Fligner procedure. **c** Significant difference was detected on K-W test ($p < 0.05$): †significantly lower ($p < 0.05$),

intoxication-2 vs. other groups on Steel-Dwass-Critchlow-Fligner procedure. **d** There was no significant difference among the groups on K-W test ($p > 0.05$). CNRQ, calibrated normalized relative quantity; As, mechanical asphyxia; Injury-1, brain injury; Injury-2, non-brain injury; Injury-3, sharp instrument injury; Intoxication-1, carbon monoxide; Intoxication-2, methamphetamine; Intoxication-3, phenobarbital

changes involved in the death process which cannot be detected directly by morphology.

Up-regulations of MMP2 and MMP9 in the brain can increase BBB permeability by degrading the endothelial basal lamina of the BBB, which results in vasogenic edema [28]. Despite the well-documented neurotoxic effects, the impact of METH on the BBB has been overlooked, and the probable mechanism has not been fully addressed.

In the present study, using mRNA measurements of cerebral MMPs, METH intoxication cases had evidently higher CNRQ values of MMP9, while phenobarbital intoxication cases showed significantly lower CNRQ values of MMP2. These findings suggest independent contributions of MMP2 and MMP9 in the brain tissues of intoxication cases, which require further investigation.

MMP9 was thought to be a key player in METH-induced alteration of BBB permeability. Several studies in animal models have shown that METH increases BBB permeability by up-regulating MMP9 after METH administration [2, 29, 30]. Both inhibiting MMP9 and deleting MMP9 gene can attenuate the BBB disruption [31, 32]. MMP-9 can digest TJ proteins of BBB. Microvascular endothelial cells of human

brain treated with METH demonstrated a decrease in CLDN5 expression, suggesting that TJ alteration may be the cause of METH-induced BBB permeability [33]. In the present study, METH intoxication cases showed lower CNRQ values of CLDN5, indicating that the increase of MMP9 may lead to the degradation of CLDN5, which can be responsible for the opening of the BBB.

Of note, characteristic findings were detected for AQP4 CNRQ values, which were higher in METH intoxication cases. To our knowledge, this is the first report showing that METH can up-regulate AQP4. As mentioned above, METH-induced up-regulation of MMP9 can increase BBB permeability, resulting in vasogenic edema. In the vasogenic edema resolution phase, an increase of AQP4 was observed in some studies [34, 35]. Therefore, in METH intoxication cases, AQP4 seems to play a beneficial role in eliminating accumulating water from the extracellular space of the CNS, suggesting an activation of the self-protective system after METH intoxication in CNS.

On the one hand, the increase of BBB deterioration by METH can accelerate transmigration of the neurotropic fungus *Cryptococcus neoformans* into the brain parenchyma after

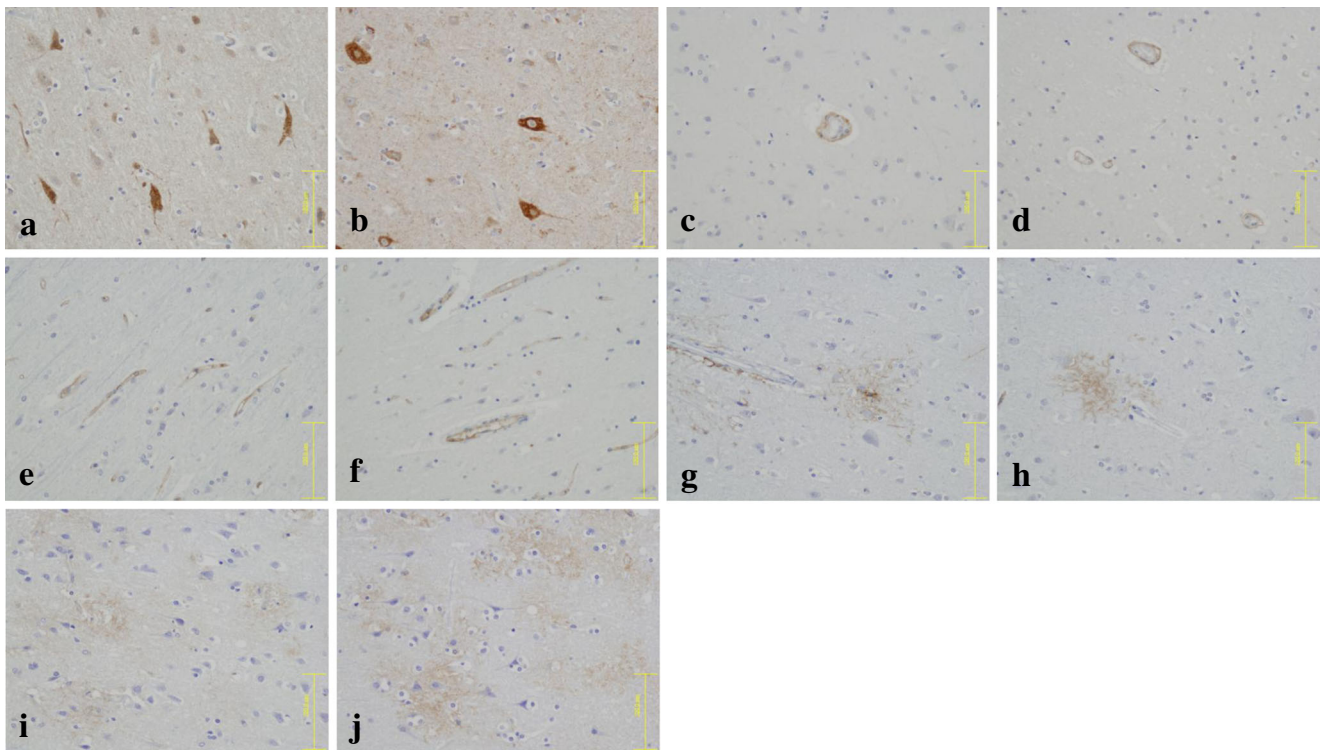


Fig. 2 Immunostaining of MMP2 (a and b) and MMP9 (c and d), CLDN5 (e and f), AQP1 (g and h) and AQP4 (i and j) in the brain. METH intoxication (a, d, f, h, and j), a 45-year-old male, survival time

6 h, 30 h postmortem. Phenobarbital intoxication (b), a 24-year-old female, survival time 6 h, 25 h postmortem. Mechanical asphyxia (c, e, g, and i), a 64-year-old male, survival time <0.5 h, 21 h postmortem

systemic infection [36]. On the other hand, METH temporarily opens the BBB and therefore may be useful as a novel therapeutic strategy to allow drugs/chemicals cross the BBB and entry into brain [37]. Therefore, the METH-induced BBB opening should be addressed from a dialectic point of view.

In the present study, the immunostaining did not detect any evident differences in distribution or intensity among all the causes of death. These findings may be because of the lower sensitivity of immunostaining in detecting changes in gene products than that with quantitative analyses of gene expressions using RT-qPCR.

The major limitation of the present study is that the integrity of the extracted RNA has not been checked prior to cDNA synthesis, though RT-qPCR performance was affected by RNA integrity [26]. RNA quality from brain tissue might be seriously affected in cases of brain damage. Both reference genes and target genes were affected by impaired RNA integrity. Our previous studies showed that postmortem degradation profiles of some target genes were similar to reference genes [38] and high correlations among some commonly used housekeeping genes using human postmortem lung tissue [39]. Indeed, patterns of RNA degradation have yet to be fully illuminated. Further cooperation and investigation may be needed to evaluate the accuracy of relative quantification, using absolute quantification.

In conclusion, the present study, using postmortem autopsy brain tissues, suggests that METH-induced increase of BBB permeability is mediated by up-regulation of MMP9 and down-regulation of CLDN5. Systematic analysis of gene expressions using RT-qPCR is a useful procedure in forensic death investigation.

Acknowledgments All practical work was performed at the Department of Legal Medicine Osaka City University.

This work was partially funded by Grants-in-Aid for Scientific Research from the Japan Society for the Promotion of Science and the Ministry of Education, Culture, Sports, Science and Technology, Japan (grant nos. 21790612 and 22590642).

References

- Halpin LE, Collins SA, Yamamoto BK (2013) Neurotoxicity of methamphetamine and 3,4-methylenedioxymethamphetamine. *Life Sci*
- Martins T, Baptista S, Goncalves J, Leal E, Milhazes N, Borges F, Ribeiro CF, Quintela O, Lendoiro E, Lopez-Rivadulla M, Ambrosio AF, Silva AP (2011) Methamphetamine transiently increases the blood-brain barrier permeability in the hippocampus: role of tight junction proteins and matrix metalloproteinase-9. *Brain Res* 1411: 28–40
- Sharma HS, Kiyatkin EA (2009) Rapid morphological brain abnormalities during acute methamphetamine intoxication in the rat: an

- experimental study using light and electron microscopy. *J Chem Neuroanat* 37(1):18–32
4. Woessner JF Jr (1994) The family of matrix metalloproteinases. *Ann N Y Acad Sci* 732:11–21
 5. Agrawal SM, Lau L, Yong VW (2008) MMPs in the central nervous system: where the good guys go bad. *Semin Cell Dev Biol* 19(1):42–51
 6. Furuse M, Tsukita S (2006) Claudins in occluding junctions of humans and flies. *Trends Cell Biol* 16(4):181–188
 7. Zador Z, Bloch O, Yao X, Manley GT (2007) Aquaporins: role in cerebral edema and brain water balance. *Prog Brain Res* 161:185–194
 8. Wang Q, Ishikawa T, Michiue T, Zhu BL, Guan DW, Maeda H (2013) Molecular pathology of brain edema after severe burns in forensic autopsy cases with special regard to the importance of reference gene selection. *Int J Legal Med* 127(5):881–889
 9. Wang Q, Ishikawa T, Michiue T, Zhu BL, Maeda H (2011) Evaluation of human brain damage in fire fatality by quantification of basic fibroblast growth factor (bFGF), glial fibrillary acidic protein (GFAP) and single-stranded DNA (ssDNA) immunoreactivities. *Forensic Sci Int* 211(1–3):19–26
 10. Maeda H, Fukita K, Oritani S, Ishida K, Zhu BL (1997) Evaluation of post-mortem oxymetry with reference to the causes of death. *Forensic Sci Int* 87(3):201–210
 11. Oritani S, Nagai K, Zhu BL, Maeda H (1996) Estimation of carboxyhemoglobin concentrations in thermo-coagulated blood on a CO-oximeter system: an experimental study. *Forensic Sci Int* 83(3):211–218
 12. Tominaga M, Michiue T, Ishikawa T, Kawamoto O, Oritani S, Ikeda K, Ogawa M, Maeda H (2013) Postmortem analyses of drugs in pericardial fluid and bone marrow aspirate. *J Anal Toxicol* 37(7):423–429
 13. Wang Q, Ishikawa T, Michiue T, Zhu BL, Guan DW, Maeda H (2012) Stability of endogenous reference genes in postmortem human brains for normalization of quantitative real-time PCR data: comprehensive evaluation using geNorm, NormFinder, and BestKeeper. *Int J Legal Med* 126(6):943–952
 14. Zhao S, Fernald RD (2005) Comprehensive algorithm for quantitative real-time polymerase chain reaction. *J Comput Biol* 12(8):1047–1064
 15. Hellemans J, Mortier G, De Paep A, Speleman F, Vandesompele J (2007) qBase relative quantification framework and software for management and automated analysis of real-time quantitative PCR data. *Genome Biol* 8(2):R19
 16. Livak KJ, Schmittgen TD (2001) Analysis of relative gene expression data using real-time quantitative PCR and the 2⁻(Delta Delta C(T)) Method. *Methods* 25(4):402–408
 17. Huth A, Vennemann B, Fracasso T, Lutz-Bonengel S, Vennemann M (2013) Apparent versus true gene expression changes of three hypoxia-related genes in autopsy derived tissue and the importance of normalisation. *Int J Legal Med* 127(2):335–344
 18. Wang Q, Ishikawa T, Michiue T, Zhu BL, Guan DW, Maeda H (2012) Quantitative immunohistochemical analysis of human brain basic fibroblast growth factor, glial fibrillary acidic protein and single-stranded DNA expressions following traumatic brain injury. *Forensic Sci Int* 221(1–3):142–151
 19. Wang Q, Ishikawa T, Michiue T, Zhu BL, Guan DW, Maeda H (2012) Evaluation of human brain damage in fatalities due to extreme environmental temperature by quantification of basic fibroblast growth factor (bFGF), glial fibrillary acidic protein (GFAP), S100beta and single-stranded DNA (ssDNA) immunoreactivities. *Forensic Sci Int* 219(1–3):259–264
 20. Hollander M, Wolfe DA (1999) Nonparametric statistical methods. Wiley series in probability and statistics Texts and references section, 2nd edn. Wiley, New York
 21. Gibbons JD, Chakraborti S (2011) Nonparametric statistical inference. Statistics, textbooks & monographs, 5th edn. Taylor & Francis, Boca Raton
 22. Madea B, Saukko P, Oliva A, Musshoff F (2010) Molecular pathology in forensic medicine-introduction. *Forensic Sci Int* 203(1–3):3–14
 23. Maeda H, Ishikawa T, Michiue T (2011) Forensic biochemistry for functional investigation of death: concept and practical application. *Leg Med (Tokyo)* 13(2):55–67
 24. Koppelkamm A, Vennemann B, Fracasso T, Lutz-Bonengel S, Schmidt U, Heinrich M (2010) Validation of adequate endogenous reference genes for the normalisation of qPCR gene expression data in human post mortem tissue. *Int J Legal Med* 124(5):371–380
 25. Kimura A, Ishida Y, Hayashi T, Nosaka M, Kondo T (2011) Estimating time of death based on the biological clock. *Int J Legal Med* 125(3):385–391
 26. Koppelkamm A, Vennemann B, Lutz-Bonengel S, Fracasso T, Vennemann M (2011) RNA integrity in post-mortem samples: influencing parameters and implications on RT-qPCR assays. *Int J Legal Med* 125(4):573–580
 27. Chen JH, Michiue T, Ishikawa T, Maeda H (2012) Molecular pathology of natriuretic peptides in the myocardium with special regard to fatal intoxication, hypothermia, and hyperthermia. *Int J Legal Med* 126(5):747–756
 28. Zhang H, Adwanikar H, Werb Z, Noble-Haesslein LJ (2010) Matrix metalloproteinases and neurotrauma: evolving roles in injury and reparative processes. *Neuroscientist* 16(2):156–170
 29. Liu Y, Brown S, Shaikh J, Fishback JA, Matsumoto RR (2008) Relationship between methamphetamine exposure and matrix metalloproteinase 9 expression. *Neuroreport* 19(14):1407–1409
 30. Urrutia A, Rubio-Araiz A, Gutierrez-Lopez MD, ElAli A, Herrmann DM, O'Shea E, Colado MI (2013) A study on the effect of JNK inhibitor, SP600125, on the disruption of blood-brain barrier induced by methamphetamine. *Neurobiol Dis* 50:49–58
 31. Rosenberg GA, Estrada EY, Dencoff JE (1998) Matrix metalloproteinases and TIMPs are associated with blood-brain barrier opening after reperfusion in rat brain. *Stroke* 29(10):2189–2195
 32. Svedin P, Hagberg H, Savman K, Zhu C, Mallard C (2007) Matrix metalloproteinase-9 gene knock-out protects the immature brain after cerebral hypoxia-ischemia. *J Neurosci* 27(7):1511–1518
 33. Ramirez SH, Potula R, Fan S, Eidem T, Papugani A, Reichenbach N, Dykstra H, Weksler BB, Romero IA, Couraud PO, Persidsky Y (2009) Methamphetamine disrupts blood-brain barrier function by induction of oxidative stress in brain endothelial cells. *J Cereb Blood Flow Metab* 29(12):1933–1945
 34. Tourdias T, Mori N, Dragonu I, Cassagno N, Boiziau C, Aussudre J, Brochet B, Moonen C, Petry KG, Dousset V (2011) Differential aquaporin 4 expression during edema build-up and resolution phases of brain inflammation. *J Neuroinflammation* 8:143
 35. Fukuda AM, Pop V, Spagnoli D, Ashwal S, Obenaus A, Badaut J (2012) Delayed increase of astrocytic aquaporin 4 after juvenile traumatic brain injury: possible role in edema resolution? *Neuroscience* 222:366–378
 36. Eugenin EA, Greco JM, Frases S, Nosanchuk JD, Martinez LR (2013) Methamphetamine alters blood brain barrier protein expression in mice, facilitating central nervous system infection by neurotropic *Cryptococcus neoformans*. *J Infect Dis* 208(4):699–704
 37. Kast RE (2009) Use of FDA approved methamphetamine to allow adjunctive use of methylnaltrexone to mediate core anti-growth factor signaling effects in glioblastoma. *J Neurooncol* 94(2):163–167
 38. Zhao D, Zhu BL, Ishikawa T, Quan L, Li DR, Maeda H (2006) Real-time RT-PCR quantitative assays and postmortem degradation profiles of erythropoietin, vascular endothelial growth factor and hypoxia-inducible factor 1 alpha mRNA transcripts in forensic autopsy materials. *Leg Med (Tokyo)* 8(2):132–136
 39. Miyazato T, Ishikawa T, Michiue T, Maeda H (2012) Molecular pathology of pulmonary surfactants and cytokines in drowning compared with other asphyxiation and fatal hypothermia. *Int J Legal Med* 126(4):581–587